Desalination and Water Treatment
www.deswater.com

doi: 10.1080/19443994.2015.1014858

57 (2016) 7079–7084
March

Taylor & Francis
Taylor & Francis Group

Morphologically controlled synthesis of porous Mn_2O_3 microspheres and their catalytic applications on the degradation of methylene blue

Ping Tao, Mihua Shao, Chengwen Song*, Chen Li, Yanyan Yin, Shuaihua Wu, Murong Cheng, Zhi Cui

School of Environment Science and Engineering, Dalian Maritime University, 1 Linghai Road, Dalian 116026, China, Tel./Fax +86 411 84724342; emails: taopingdlmu@163.com (P. Tao), mihuashao@126.com (M. Shao), chengwensong@dlmu.edu.cn (C. Song), li_chen100@163.com (C. Li), yanyanyin@yeah.net (Y. Yin), shuaihuawu@yeah.net (S. Wu), murongcheng@yeah.net (M. Cheng), zhicui1988@126.com (Z. Cui)

Received 9 May 2014; Accepted 26 January 2015

ABSTRACT

Porous Mn_2O_3 microspheres are controllably synthesized by selectively etching $MnCO_3$ precursor with HCl solution. Morphologies and microstructures of Mn_2O_3 microspheres are analyzed by SEM, TEM, XRD, and N_2 sorption technique. The catalytic performances of Mn_2O_3 microspheres for the degradation of methylene blue (MB) are investigated, and the reaction kinetics of MB degradation is also studied. The results show it is feasible to control the morphologies of Mn_2O_3 microspheres by adjusting the concentration of HCl solution, and the well-developed porous Mn_2O_3 microspheres demonstrate good potential on MB degradation. The degradation reactions follow the pseudo-first-order kinetic model, and the degradation capabilities for MB are great dependent on BET surface areas and pore volumes of Mn_2O_3 microspheres.

Keywords: Porous; Mn_2O_3; Nanostructures; Degradation

1. Introduction

Water pollution caused by various industrial effluents, agricultural runoff, and chemical spills has become a crucial issue in the recent years with the rapid growth of the world population, industrialization, unplanned urbanization, and agricultural activities [1,2]. Wastewaters from dyeing and other textile processes, containing high levels of color, refractory organics, and solids, pose a significant threat to environment and public health owing to their potential to form toxic aromatic products with carcinogenic and mutagenic properties [3,4]. Methylene blue (MB) is the most commonly employed basic dye, which can cause increased heart rate, vomiting, shock, Heinz body formation, cyanosis, jaundice, quadriplegia, and tissue necrosis in humans [5]. Various methods, including adsorption, ion-exchange, coagulation/flocculation, membrane separation and advanced oxidation processes (AOPs) have been applied for the treatment of dye wastewaters [6,7]. Of the above-mentioned treatment techniques, AOPs are regarded as the most effective approaches to decontaminate dye wastewaters based on the generation of reactive species in the presence of catalysts, which can degrade a broad range of organic pollutants quickly and non-selectively [8]. Many metal oxides, such as TiO_2, CuO, ZnO, Fe_2O_3, and Mn_2O_3, have been used as catalysts for the

*Corresponding author.

degradation of dye wastewaters due to their unique physical and chemical properties [9,10]. Among them, Mn_2O_3, is an inexpensive, environment friendly metal oxide, has attracted considerable attention because of its distinctive properties and extensive applications in catalysis, adsorption, ion-exchange materials, and Li-ion batteries. Up to now, Mn_2O_3 nanostructures with a variety of morphologies including rods, wires, or cubes have been successfully synthesized [11]. As we known, the morphologies of nanomaterials have great effect on their catalytic activities, and porous and hollow nanostructures are more beneficial to enhance the degradation capability of Mn_2O_3 nanomaterials because of their large specific surface areas, high porosities, and low densities [12]. At present, porous and hollow Mn_2O_3 are usually fabricated using $MnCO_3$ as a precursor. Cao et al. selectively oxidized $MnCO_3$ to form sandwiched microspheres firstly and then removed unoxidized $MnCO_3$ middle layer by HCl solution. After heat treatment, double-shelled Mn_2O_3 hollow spheres were obtained and used for the treatment of phenol wastewater [13]. Qiao et al. prepared hollow and double-shelled Mn_2O_3 microspheres as a superior anode material using similar methods [14]. Liu et al. directly annealed $MnCO_3$ hollow cubes to prepare Mn_2O_3 hollow cubes and investigated their catalytic performance for CO oxidation [15]. Based on these works, we develop a facile method for the controlled synthesis of porous Mn_2O_3 microspheres by selectively etching $MnCO_3$ precursor with HCl solution. The morphologies of porous Mn_2O_3 microspheres are readily tunable by changing the concentration of HCl solution. The catalytic performance of porous Mn_2O_3 microspheres is also investigated to evaluate their potential in MB removal from wastewater.

2. Experimental

2.1. Synthesis of porous Mn_2O_3 microspheres

Seventy milliliters of manganese sulfate solution (0.07 M) was mixed with 20 mL of ethanol under stirring, and 70 mL of sodium hydrogen carbonate solution (0.715 M) was added dropwise to the above mixture. The mixture was vigorously stirred for 30 min followed by centrifugation (4,000 rpm, 5 min), and $MnCO_3$ microspheres were obtained subsequently. Then, 20 mL of deionized water was added to the solid precipitate. The mixture was vigorously stirred for 10 min, and then, 10 mL of HCl solution (0.10, 0.14, and 0.18 M, respectively) was added dropwise to the above solution. After washing with distilled water, the product was calcined at 500°C for 10 h to get porous Mn_2O_3 microspheres.

2.2. Characterizations of porous Mn_2O_3 microspheres

The porous structure of Mn_2O_3 microspheres was characterized by nitrogen sorption technique (Quantachrome Autosorb-iQ). The morphologies of Mn_2O_3 microspheres were observed by SEM (Philips XL30 FEG) and TEM (FEI/Philips Techal 12 BioTWIN). X-ray diffraction (XRD) patterns of Mn_2O_3 microspheres were recorded using a D/Max-2400 diffractometer (Cu Kα radiation, $\lambda = 1.54055$ Å) in a range of diffraction angle 2θ from 10 to 80° to analyze the diffraction peaks of Mn_2O_3 microspheres.

2.3. MB degradation

0.1 g of Mn_2O_3 microspheres was dispersed in 100 mL of MB aqueous solution (20 mg/L). Then, 2 mL of aqueous H_2O_2 (30 wt.%) was added into the reaction mixture. The catalytic reaction was performed under magnetic stirring at 25°C for 5 h. The mixture of catalyst and MB solution was centrifuged for a given time interval. Then, 2 mL of supernatant solution was analyzed immediately using an UV–visible spectrophotometer.

The degree of MB degradation (D) was estimated by the following equation:

$$D = \frac{C_0 - C_t}{C_0} \times 100\% \quad (1)$$

where C_0 (mg/L) is the initial concentration of MB and C_t (mg/L) is the concentration of MB at time t during the catalytic reaction.

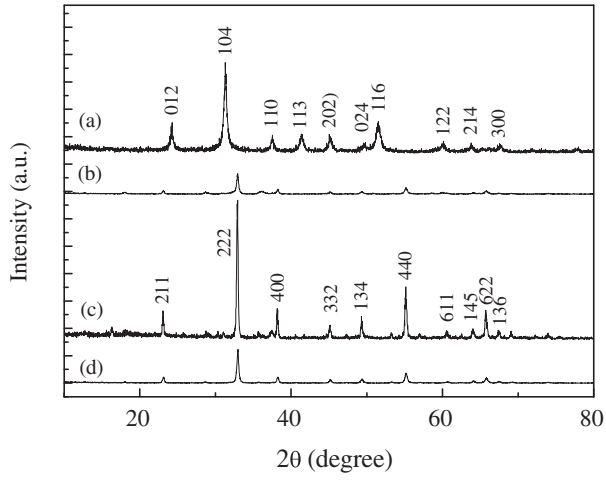

Fig. 1. XRD patterns of (a) $MnCO_3$, (b) Mn_2O_3-010, (c) Mn_2O_3-014, and (d) Mn_2O_3-018.

The pseudo-first-order kinetics was expressed in terms of Langmuir–Hinshelwood (L–H) model [16].

$$\ln\left(\frac{C}{C_0}\right) = kt \quad (2)$$

where k is the pseudo-first-order rate constant.

3. Results and discussion

3.1. Morphologies and microstructure of Mn_2O_3 microspheres

Fig. 1(a) presents the typical XRD patterns of $MnCO_3$ precursor, which can be indexed as a pure rhombohedral $MnCO_3$ (JCPDS No. 83-1763). Fig. 1(b–d) provides the XRD patterns of the resulting Mn_2O_3 microspheres etched by 0.10, 0.14, and 0.18 M HCl. All of the diffraction peaks correspond to pure Mn_2O_3 (JCPDS No. 89-4836) [17]. We also notice that the three types of Mn_2O_3 microspheres show different peak intensities, which may be related to the morphologies of Mn_2O_3 microspheres etched by HCl solution with different concentrations [18]. Among them, the Mn_2O_3 microspheres etched by 0.14 M HCl demonstrate the strongest peak intensity, suggesting that the sample has good crystallinity.

Fig. 2(a) is a typical SEM image of $MnCO_3$ microspheres. A dense spherical morphology with a uniform size distribution ranging from 350 to 450 nm is observed. Fig. 2(b) shows a SEM image of Mn_2O_3 microspheres synthesized by etching with 0.10 M

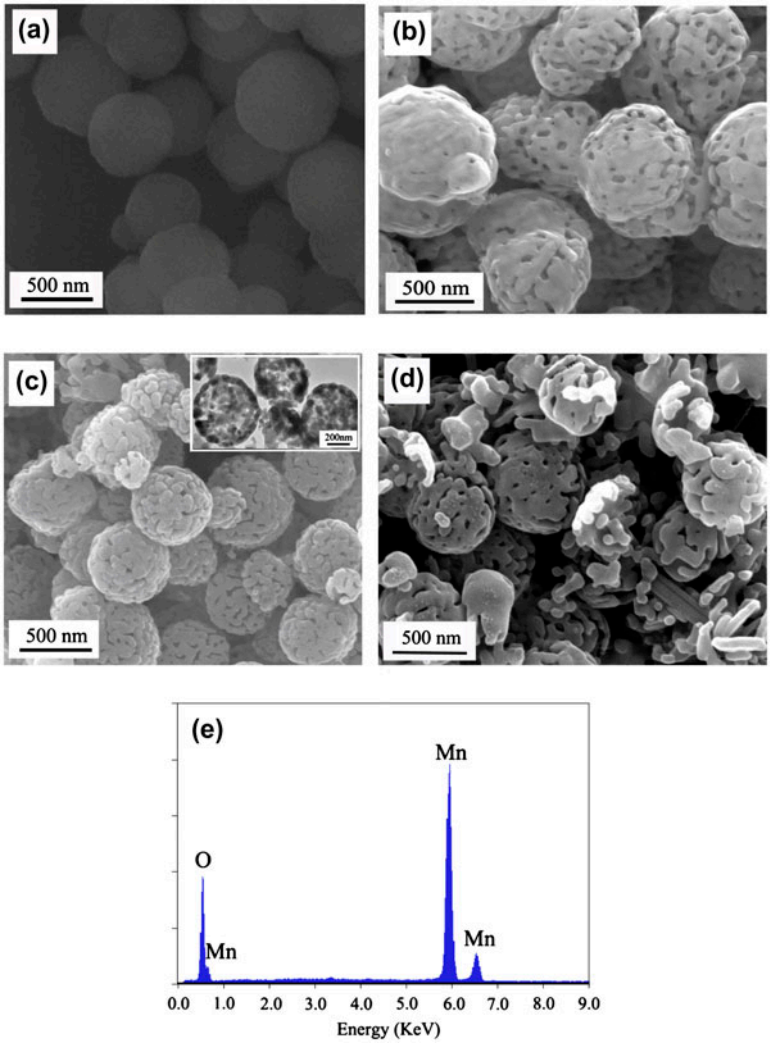

Fig. 2. SEM images of (a) $MnCO_3$ (b) Mn_2O_3-010, (c) Mn_2O_3-014, and (d) Mn_2O_3-018, TEM image (Inset) and EDAX (e) of Mn_2O_3-014.

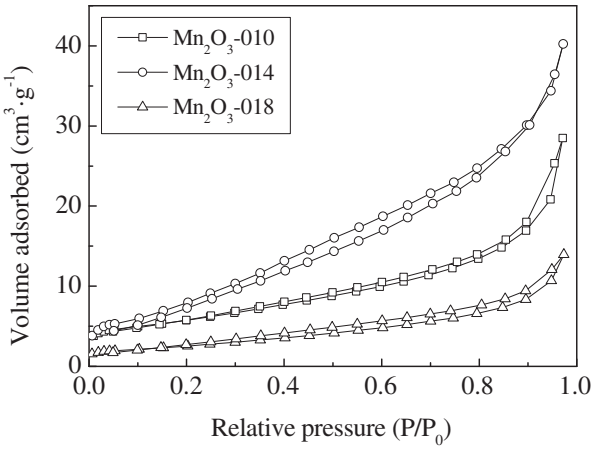

Fig. 3. N_2 adsorption isotherm of Mn_2O_3-014.

HCl. Obviously, the porous structure of Mn_2O_3 microspheres is not well developed due to insufficient etchant. Increasing HCl concentration to 0.14 M, Mn_2O_3 microspheres with rich porous structure are formed (as shown in Fig. 2(c)). The corresponding TEM image (Fig. 2(c) inset) proves that the sample is porous structure with the shell thickness of ca. 20 nm. When the concentration of HCl solution reaches 0.18 M, more fragments of Mn_2O_3 microspheres are observed owing to excessive dosage of HCl. The reason that the $MnCO_3$ microspheres can be selectively etched by HCl solution and form porous structure ultimately is attributed to the special core–shell structure of $MnCO_3$ microspheres synthesized by this method [13]. The chemical composition of the as-prepared Mn_2O_3 microspheres is further confirmed by EDAX analysis. The spectrum shows two strong signals of Mn and O (Fig. 2(d)). The amounts of Mn and O in the Mn_2O_3 sample are 39.1 and 60.9 at.%, which is close to the stoichiometric composition of Mn_2O_3, indicating that the as-prepared porous microspheres are Mn_2O_3 rather than other manganese oxides. The result agrees with the XRD analysis.

N_2 adsorption isotherm of porous Mn_2O_3 microspheres is presented in Fig. 3. The adsorption isotherm shows a type IV curve with a hysteresis loop, illustrating this sample has typical mesoporous structure [19]. As we know, BET surface area, pore volume, and average pore diameter have direct relationships with the development of porous materials. Table 1 shows the pore structure properties of Mn_2O_3 microspheres. The increase of HCl concentration from

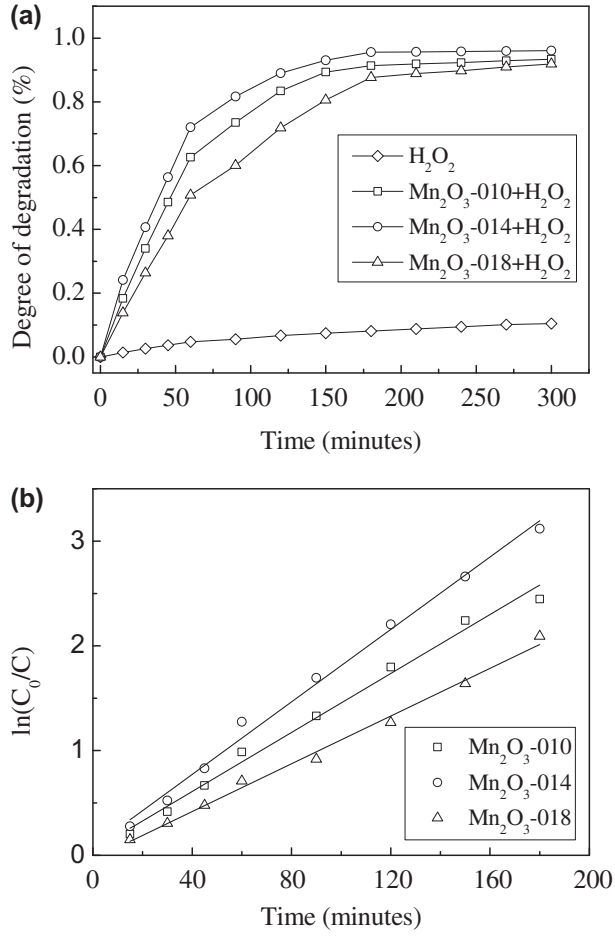

Fig. 4. (a) Time profiles of MB degradation and (b) Pseudo-first-order kinetic plots of $\ln(C_0/C)$ vs. time of MB degradation using Mn_2O_3 microspheres synthesized in this work.

Table 1
Pore structure properties of porous Mn_2O_3 microspheres

Samples	BET surface area[a] ($m^2 g^{-1}$)	Pore diameter[b] (nm)	Pore volume[b] ($cm^3 g^{-1}$)
Mn_2O_3-010	20.59	2.184	0.044
Mn_2O_3-014	33.73	2.452	0.070
Mn_2O_3-018	14.56	2.216	0.023

[a]Calculated by the BET method.
[b]Calculated by the BJH method from desorption.

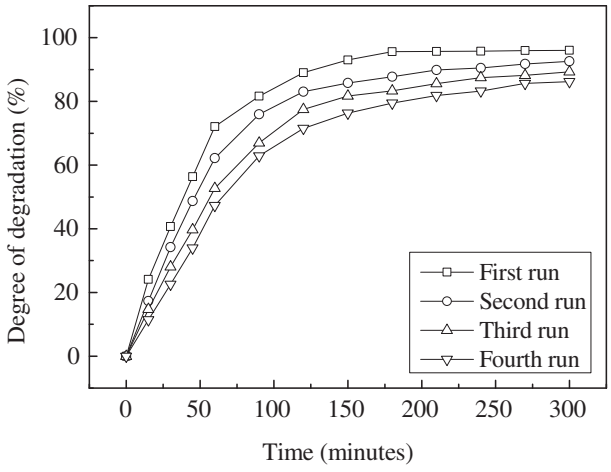

Fig. 5. Recyclability tests of Mn_2O_3-014 in MB degradation.

0.10 to 0.14 M promotes the improvements of the BET surface area (from 20.59 to 33.73 m^2/g), pore volume (from 0.044 to 0.070 cm^3/g), and average pore diameter (from 2.184 to 2.452 nm), producing more rich porous structure in Mn_2O_3 microspheres, which is consistent with SEM analysis. With the further increase of HCl concentration to 0.18 M, BET surface area, pore volume, and average pore diameter decrease to 14.56 m^2/g, 0.023 cm^3/g, and 2.216 nm, respectively, which agree with the fact that the porous structure of Mn_2O_3 microspheres is destroyed by excessive HCl solution.

3.2. Catalytic degradation of MB

The potential capabilities of degrading MB from wastewater using porous Mn_2O_3 microspheres are investigated. As shown in Fig. 4(a), the degradation reaction of MB is very slow using H_2O_2 in the absence of porous Mn_2O_3 microspheres and the degradation degree of MB only reaches 10.48% for 300 min. This indicates that H_2O_2 is not effective in degrading the stable MB. When both Mn_2O_3 microspheres and H_2O_2 are used to treat MB solution, the degradation degree of MB increases sharply in the initial stage and then gradually remains steady after 180 min. The three kinds of Mn_2O_3 microspheres exhibit different capabilities for MB degradation, which is related to the pore structure properties of Mn_2O_3 microspheres. The sample with large BET surface area and pore volume generally demonstrates high catalytic performance in degrading MB, and thus, much more amount of MB is removed from the wastewater. Those indicate that high BET surface area and pore volume are beneficial for MB degradation.

Fig. 4(b) displays the plots of $\ln(\frac{C_0}{C})$ vs. t for MB degradation by three kinds of Mn_2O_3 microspheres. It is obvious that they all follow linear relationships, suggesting that the degradation reactions obey the pseudo-first-order kinetic model. The rate constants are estimated to follow the order of 0.018 min^{-1} (Mn_2O_3-014) > 0.014 min^{-1} (Mn_2O_3-010) > 0.011 min^{-1} (Mn_2O_3-018), which indicates that the catalytic performances of Mn_2O_3 microspheres are in good agreement with the order of their BET surface areas and pore volumes.

In order to evaluate the reusability of porous Mn_2O_3 microspheres, four consecutive degradation experiments are performed. As shown in Fig. 5, the porous Mn_2O_3 microspheres exhibit no significant loss on degradation abilities after four cycles and the degradation degree of MB still can reach 86.23% for 100 mL of 20 mg/L MB solutions, suggesting the porous Mn_2O_3 microspheres are recyclable catalysts for the MB degradation. Compared to other catalysts reported in the literature shown in Table 2, the degree of MB degradation using the porous Mn_2O_3 microspheres synthesized in this work is higher than other catalysts (expect 97% degradation degree by elongated α-Fe_2O_3). These clearly indicate that the porous Mn_2O_3 microspheres prepared by solvothermal method in this paper are promising catalysts for MB degradation.

Table 2
Comparison of MB degradation degree of Mn_2O_3 with that of other catalysts reported in the literature

Catalysts	MB concentration (mg/L)	The degree of degradation (%)	Reference
Porous Mn_2O_3 microspheres	20	96.05	In this work
Core–shell Mn_2O_3	15	~48	[20]
MnO_2 nanopincers	20	90.2	[21]
α-Fe_2O_3 nanoparticles	10	80	[22]
Spherical α-Fe_2O_3	20	51	[23]
Elongated α-Fe_2O_3	20	97	[23]

4. Conclusions

Morphologies of porous Mn_2O_3 microspheres are successfully controlled by selectively etching $MnCO_3$ precursor by HCl solution. The investigation on catalytic performances of as-prepared Mn_2O_3 microspheres demonstrates that high degradation degree of MB is obtained using Mn_2O_3 microspheres as catalysts in the presence of H_2O_2. The capabilities for MB degradation are directly related to the pore structure properties of Mn_2O_3 microspheres, and high BET surface area and pore volume can enhance the catalytic performances of Mn_2O_3 microspheres in degrading MB. The degradation reactions of MB are represented by pseudo-first-order kinetic model.

Acknowledgments

This work was supported by the National Natural Science Foundation of China (21276035, 21476034), Sub-project of Central Sharing Funds for using sea area (2013-348-7), Special Foundation for Ocean Environmental Protection of Ocean and Fisheries Department of Liaoning Province (2012-Inhyhbc-0004, 2012-Inhyhbc-005), the Scientific Research Project of Education Department of Liaoning Province (L2013203), the Natural Science Foundation of Liaoning Province (2014025014), and the Fundamental Research Funds for the Central Universities (3132015219).

References

[1] M. Vakili, M. Rafatullah, B. Salamatinia, A.Z. Abdullah, M.H. Ibrahim, K.B. Tan, Z. Gholami, P. Amouzgar, Application of chitosan and its derivatives as adsorbents for dye removal from water and wastewater: A review, Carbohydr. Polym. 113 (2014) 115–130.

[2] M. Qamar, M.A. Gondal, K. Hayat, Z.H. Yamani, K. Al-Hooshani, Laser-induced removal of a dye C.I. Acid Red 87 using *n*-type WO_3 semiconductor catalyst, J. Hazard. Mater. 170 (2009) 584–589.

[3] R. Yu, H. Chen, W. Cheng, Y. Lin, C. Huang, Monitoring of ORP, pH and DO in heterogeneous Fenton oxidation using nZVI as a catalyst for the treatment of azo-dye textile wastewater, J. Taiwan Inst. Chem. E. 45 (2014) 947–954.

[4] U. Kalsoom, S.S. Ashraf, M.A. Meetani, M.A. Rauf, H.N. Bhatti, Degradation and kinetics of H_2O_2 assisted photochemical oxidation of Remazol Turquoise Blue, Chem. Eng. J. 200–202 (2012) 373–379.

[5] K. Rastogi, J.N. Sahu, B.C. Meikap, M.N. Biswas, Removal of methylene blue from wastewater using fly ash as an adsorbent by hydrocyclone, J. Hazard. Mater. 158 (2008) 531–540.

[6] K. Hwang, J. Lee, W. Shim, H. Jang, S. Lee, S. Yoo, Adsorption and photocatalysis of nanocrystalline TiO_2 particles prepared by sol–gel method for methylene blue degradation, Adv. Powder Technol. 23 (2012) 414–418.

[7] C. Liang, S. Sun, F. Li, Y. Ong, T. Chung, Treatment of highly concentrated wastewater containing multiple synthetic dyes by a combined process of coagulation/flocculation and nanofiltration, J. Membr. Sci. 469 (2014) 306–315.

[8] A.R. Khataee, V. Vatanpour, A.R. Amani Ghadim, Decolorization of C.I. Acid Blue 9 solution by UV/Nano-TiO_2, fenton, fenton-like, electro-fenton and electrocoagulation processes: A comparative study, J. Hazard. Mater. 161 (2009) 1225–1233.

[9] J. Park, I. Jang, B. Kwon, S. Jang, S. Oh, Formation of manganese oxide shells on silica spheres with various crystal structures using surfactants for the degradation of methylene blue dye, Mater. Res. Bull. 48 (2013) 469–475.

[10] L. Fink, I. Dror, B. Berkowitz, Enrofloxacin oxidative degradation facilitated by metal oxide nanoparticles, Chemosphere 86 (2012) 144–149.

[11] W. Li, L. Zhang, S. Sithambaram, J. Yuan, X. Shen, M. Aindow, S.L. Suib, Shape evolution of single-crystalline Mn_2O_3 using a solvothermal approach, J. Phys. Chem. C 111 (2007) 14694–14697.

[12] J. Cao, Y. Zhu, K. Bao, L. Shi, S. Liu, Y. Qian, Microscale Mn_2O_3 hollow structures: Sphere, cube, ellipsoid, dumbbell, and their phenol adsorption properties, J. Phys. Chem. C 113 (2009) 17755–17760.

[13] J. Cao, Y. Zhu, L. Shi, L. Zhu, K. Bao, S. Liu, Y. Qian, Double-shelled Mn_2O_3 hollow spheres and their application in water treatment, Eur. J. Inorg. Chem. 2010 (2010) 1172–1176.

[14] Y. Qiao, Y. Yu, Y. Jin, Y. Guan, C. Chen, Synthesis and electrochemical properties of porous double-shelled Mn_2O_3 hollow microspheres as a superior anode material for lithiumion batteries, Electrochim. Acta 132 (2014) 323–331.

[15] L. Liu, X. Zhang, R. Wang, J. Liu, Facile synthesis of Mn_2O_3 hollow and core–shell cube-like nanostructures and their catalytic properties, Superlattices Microstruct. 72 (2014) 219–229.

[16] X. Luo, S. Zhang, X. Lin, New insights on degradation of methylene blue using thermocatalytic reactions catalyzed by low-temperature excitation, J. Hazard. Mater. 260 (2013) 112–121.

[17] Y. Deng, Z. Li, Z. Shi, H. Xu, F. Peng, G. Chen, Porous Mn_2O_3 microsphere as a superior anode material for lithium ion batteries, RSC Adv. 2 (2012) 4645–4647.

[18] M. Inoue, I. Hirasawa, The relationship between crystal morphology and XRD peak intensity on $CaSO_4{\cdot}2H_2O$, J. Cryst. Growth 380 (2013) 169–175.

[19] F. Jiao, A. Harrison, A.H. Hill, P.G. Bruce, Mesoporous Mn_2O_3 and Mn_3O_4 with crystalline walls, Adv. Mater. 19 (2007) 4063–4066.

[20] Y. Huo, Y. Zhang, Z. Xu, J. Zhu, H. Li, Preparation of Mn_2O_3 catalyst with core–shell structure via spray pyrolysis assisted with glucose, Res. Chem. Intermed. 35 (2009) 791–798.

[21] G. Cheng, L. Yu, T. Lin, R. Yang, M. Sun, B. Lan, L. Yang, F. Deng, A facile one-pot hydrothermal synthesis of β-MnO_2 nanopincers and their catalytic degradation of methylene blue, J. Solid State Chem. 217 (2014) 57–63.

[22] H. Yan, X. Su, C. Yang, J. Wang, C. Niu, Improved photocatalytic and gas sensing properties of α-Fe_2O_3 nanoparticles derived from β-FeOOH nanospindles, Ceram. Int. 40 (2014) 1729–1733.

[23] W. Tan, Y. Yu, M. Wang, F. Liu, L.K. Koopal, Shape evolution synthesis of monodisperse spherical, ellipsoidal, and elongated hematite (α-Fe_2O_3) nanoparticles using ascorbic acid, Cryst. Growth Des. 14 (2014) 157–164.